Figure S1

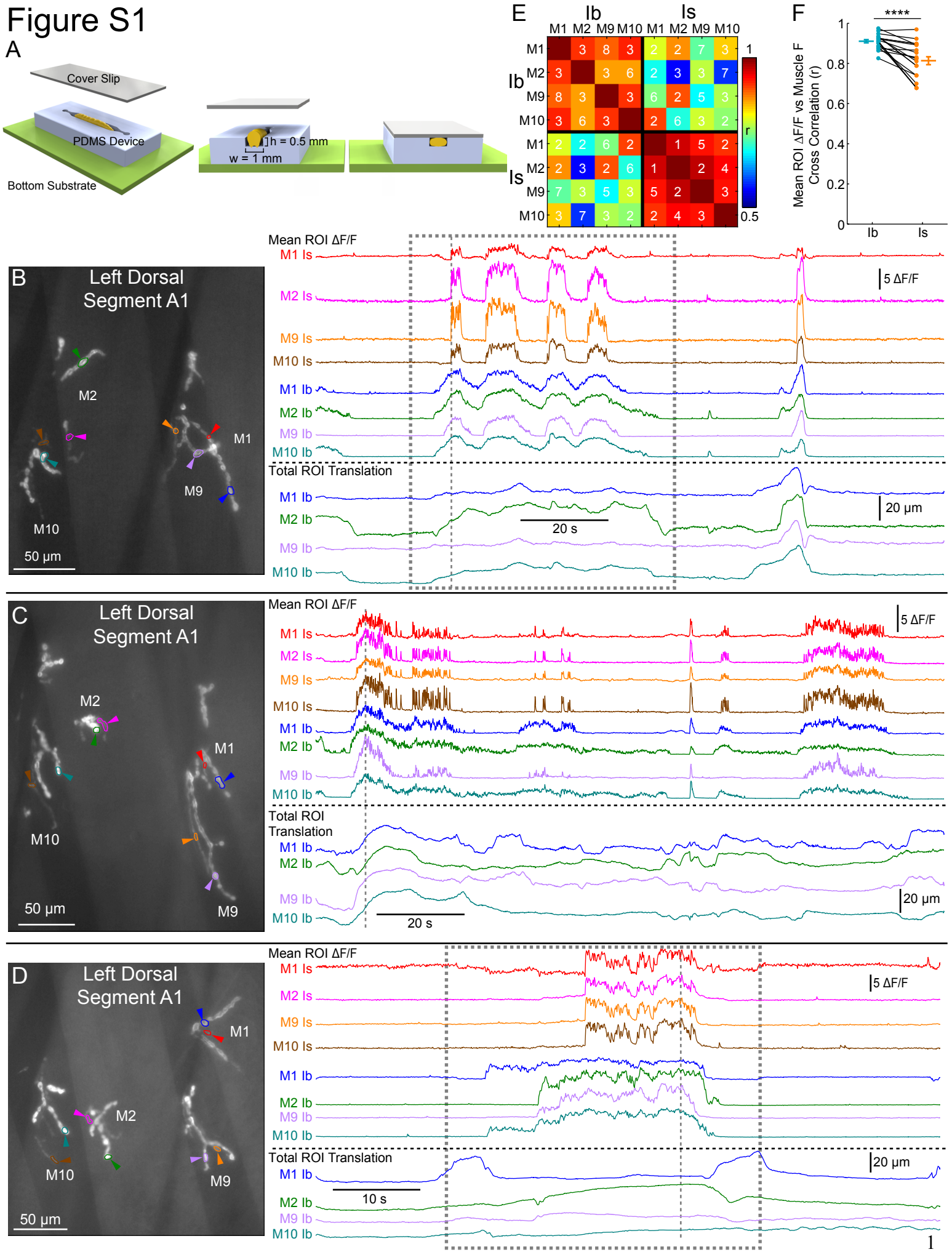
A
Cover Slip
PDMS Device
Bottom Substrate
h = 0.5 mm
w = 1 mm
E
Ib
Is
M1 M2 M9 M10 M1 M2 M9 M10
M1 3 8 3 2 2 7 3
M2 3 3 6 2 3 3 7
M9 8 3 3 6 2 5 3
M10 3 6 3 2 6 3 2
M1 2 2 6 2 1 5 2
M2 2 3 2 6 1 2 4
M9 7 3 5 3 5 2 3
M10 3 7 3 2 2 4 3
1
r
0.5
F
****
Mean ROI ΔF/F vs Muscle F
Cross Correlation (r)
1
0.8
0.6
0.4
0.2
0
Ib
Is
B
Left Dorsal
Segment A1
M2
M1
M9
M10
50 μm
Mean ROI ΔF/F
M1 Is
M2 Is
M9 Is
M10 Is
M1 Ib
M2 Ib
M9 Ib
M10 Ib
5 ΔF/F
Total ROI Translation
M1 Ib
M2 Ib
M9 Ib
M10 Ib
20 s
20 μm
C
Left Dorsal
Segment A1
M2
M1
M10
M9
50 μm
Mean ROI ΔF/F
M1 Is
M2 Is
M9 Is
M10 Is
M1 Ib
M2 Ib
M9 Ib
M10 Ib
5 ΔF/F
Total ROI
Translation
M1 Ib
M2 Ib
M9 Ib
M10 Ib
20 s
20 μm
D
Left Dorsal
Segment A1
M1
M2
M10
M9
50 μm
Mean ROI ΔF/F
M1 Is
M2 Is
M9 Is
M10 Is
M1 Ib
M2 Ib
M9 Ib
M10 Ib
5 ΔF/F
Total ROI Translation
M1 Ib
M2 Ib
M9 Ib
M10 Ib
10 s
20 μm

Figure S1. Additional *in vivo* SynapGCaMP6f analysis (Related to Figure 1)
(A) 3D rendering of the *in vivo* PDMS imaging chamber.
(B-D) (Left) Reference image and ROIs used for $\Delta F/F$ and translation calculations. (Right) *In vivo* $\Delta F/F$ recording data and translation data. Vertical gray dashed line indicates the frame corresponding to the reference image. Data in (B) corresponds to the example in Figure 1F-1G (gray dashed box region) as well as Figure 2I-2K, Figure S2 and **Supplemental Movie 2**. Data in (D) corresponds to the M10 data in Figure 2D and 2E (gray dashed box region).
(E) Pearson's cross-correlation matrix between M1-Ib, M2-Ib, M9-Ib, M10-Ib, M1-Is, M2-Is, M9-Is, M10-Is. Numbers indicate the number of comparisons.
(F) Cross-correlations between $\Delta F/F$ traces and the background muscle fluorescence (F_m). (n = 17 animals, 21 Ib NMJs and 21 Is NMJs)
Mean ± SEM indicated in relevant panels. Comparison made with Student's t-test (F). **** $p < 0.0001$.

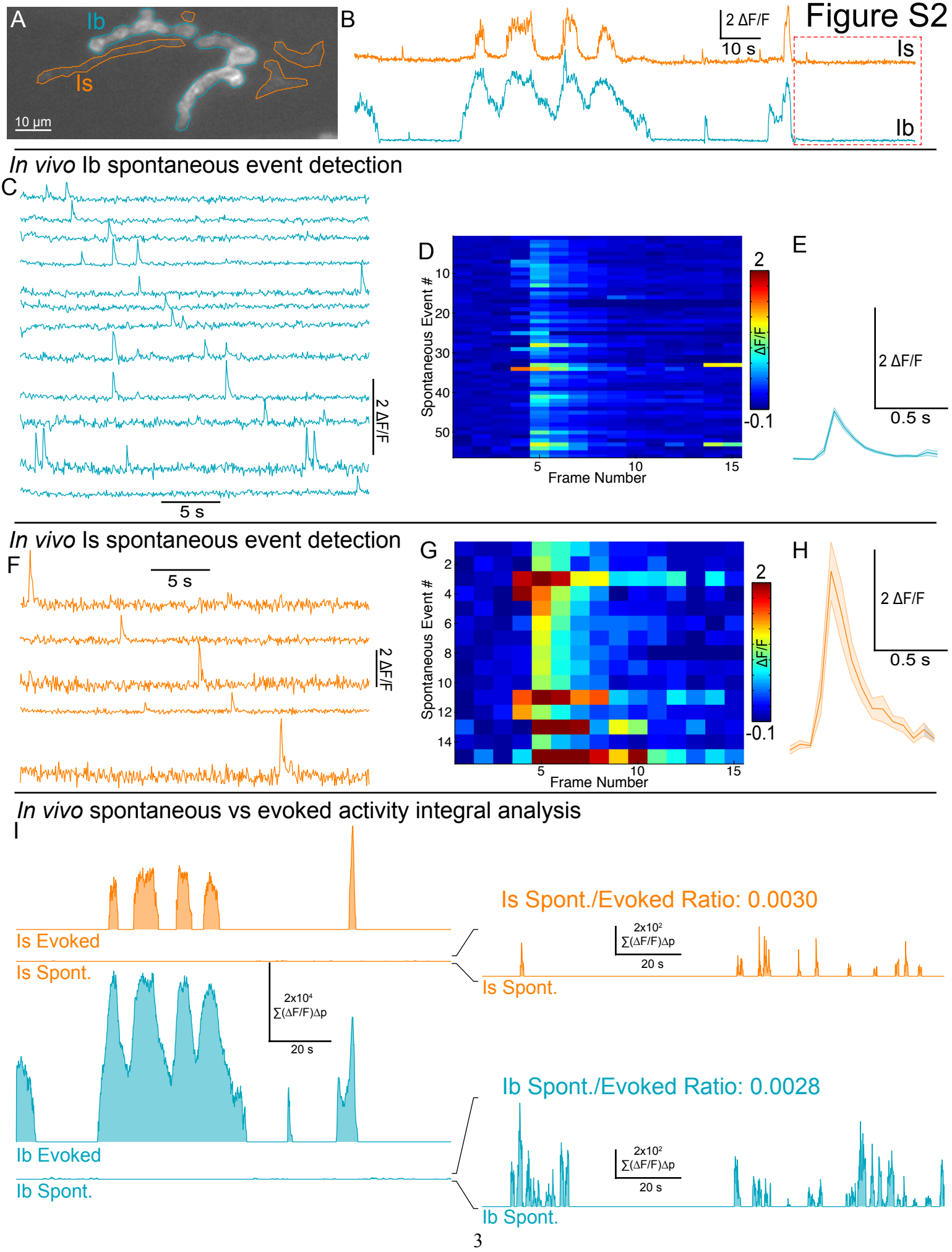
A
Ib
Is
10 µm
B
2 ΔF/F
10 s
Is
Ib
Figure S2
In vivo Ib spontaneous event detection
C
2 ΔF/F
5 s
D
Spontaneous Event #
10
20
30
40
50
5
10
15
Frame Number
2
ΔF/F
-0.1
E
2 ΔF/F
0.5 s
In vivo Is spontaneous event detection
F
5 s
2 ΔF/F
G
Spontaneous Event #
2
4
6
8
10
12
14
5
10
15
Frame Number
2
ΔF/F
-0.1
H
2 ΔF/F
0.5 s
In vivo spontaneous vs evoked activity integral analysis
I
Is Evoked
Is Spont.
2x10⁴
∑(ΔF/F)Δp
20 s
Ib Evoked
Ib Spont.
Is Spont./Evoked Ratio: 0.0030
2x10²
∑(ΔF/F)Δp
20 s
Is Spont.
Ib Spont./Evoked Ratio: 0.0028
2x10²
∑(ΔF/F)Δp
20 s
Ib Spont.

Figure S2. Additional illustration of *in vivo* spontaneous quantal release analysis (Related to Figure 2)
(A) In vivo analysis regions for Ib (blue) and Is (orange) NMJs
(B) Full single synapse $\Delta F/F$ traces corresponding to Figure 2I. Red box indicates the time window displayed in Figures S2C-S2H. Data matches example in **Supplemental Movie 3.**
(C-H) Examples of *in vivo* spontaneous quantal release analysis for Ib (C-E) and Is NMJs (F-H). Includes single synapse $\Delta F/F$ examples showing examples of spontaneous quantal events (C and F), heatmaps showing the aligned spontaneous $\Delta F/F$ amplitude data for all identified spontaneous quantal events (D and G) for this recording period (B), and mean $\Delta F/F$ waveforms (E and H) (± SEM).
(I) Example calculation of the spatial $\Delta F/F$ integral, $\Sigma(\Delta F/F)\Delta p$ at all time points for the example in Figure S2A and S2B. Traces are separated by evoked and spontaneous $\Sigma(\Delta F/F)\Delta p$ for Is (orange) and Ib (blue) NMJs. Expanded view on right shows more detailed spontaneous $\Sigma(\Delta F/F)\Delta p$ traces as well as the corresponding spontaneous/evoked total synaptic transmission ($\Sigma\Sigma(\Delta F/F)\Delta p\Delta t$) ratio.

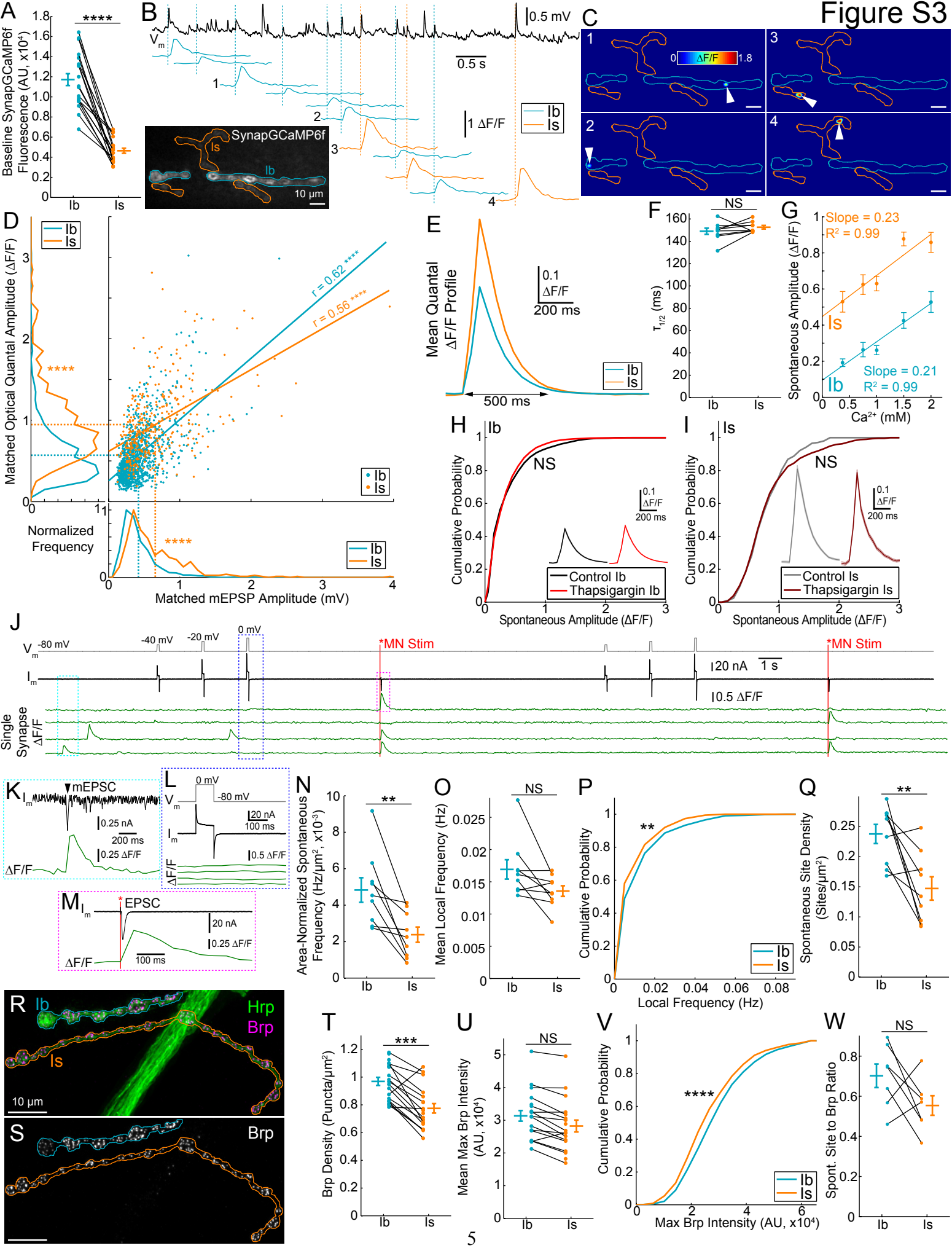
Figure S3
A
Baseline SynapGCaMP6f Fluorescence (AU, x10⁴)
****
Ib
Is
B
0.5 mV
0.5 s
1 ΔF/F
Ib
Is
SynapGCaMP6f
10 μm
C
ΔF/F
0
1.8
D
Matched Optical Quantal Amplitude (ΔF/F)
r = 0.62 ****
r = 0.56 ****
Normalized Frequency
Matched mEPSP Amplitude (mV)
E
Mean Quantal ΔF/F Profile
0.1 ΔF/F
200 ms
500 ms
F
NS
τ1/2 (ms)
G
Slope = 0.23
R² = 0.99
Slope = 0.21
R² = 0.99
Spontaneous Amplitude (ΔF/F)
Ca²⁺ (mM)
H
Ib
NS
Cumulative Probability
Control Ib
Thapsigargin Ib
Spontaneous Amplitude (ΔF/F)
I
Is
NS
Control Is
Thapsigargin Is
J
-80 mV
-40 mV
-20 mV
0 mV
*MN Stim
120 nA
1 s
0.5 ΔF/F
Single Synapse ΔF/F
K
mEPSC
0.25 nA
200 ms
0.25 ΔF/F
ΔF/F
L
0 mV
-80 mV
20 nA
100 ms
0.5 ΔF/F
M
EPSC
20 nA
0.25 ΔF/F
100 ms
N
Area-Normalized Spontaneous Frequency (Hz/μm², x10⁻³)
O
Mean Local Frequency (Hz)
P
Cumulative Probability
Local Frequency (Hz)
Q
Spontaneous Site Density (Sites/μm²)
R
Ib
Is
Hrp
Brp
10 μm
S
Brp
T
Brp Density (Puncta/μm²)
U
Mean Max Brp Intensity (AU, x10⁴)
V
Cumulative Probability
Max Brp Intensity (AU, x10⁴)
W
Spont. Site to Brp Ratio

Figure S3. Additional characterization of WT Ib and Is spontaneous release (Related to Figure 3)
(A) Mean NMJ baseline SynapGCaMP6f fluorescence. (Ib n = 21 NMJs; Is n = 20 NMJs; 18 NMJ pairs)
(B) V_m trace with matched mEPSP and $\Delta F/F$ traces for identified spontaneous quantal events at the Ib (blue) or Is (orange) NMJ. Inset shows the baseline SynapGCaMP6f fluorescence with Ib (blue) and Is (orange) NMJ borders highlighted. Note that not all mEPSPs will have a corresponding fluorescence response, as the whole Ib and Is NMJs are not in the imaging field of view.
(C) Images corresponding to four of the events indicated in Figure S3B. White arrows highlight the event locations. Example is also presented in **Supplemental Movie 5.**
(D) Matched mEPSP amplitudes (mV) versus optical amplitudes ($\Delta F/F$) along with the normalized histograms for both mEPSP amplitudes and optical amplitudes. Dotted lines correspond to mean mEPSPs amplitudes (Ib = 0.419 mV and Is = 0.654 mV) and mean optical amplitudes ($\Delta F/F$: Ib = 0.367 and Is = 0.6219). Plots include data from 31, 30s recordings at 11 different NMJs including n = 1084 matched Ib events (blue) n = 325 matched Is events (orange). Linear regression line for Ib is y=0.53x+0.2 and for Is is y=0.34x+0.4 with r values indicated on the plot.
(E) Mean spontaneous quantal $\Delta F/F$ time course for all pooled events at Ib and Is NMJs. All identified events were aligned according to their peak time and then averaged. (Ib n = 9 NMJs, 2515 pooled events; Is n = 9 NMJs, 1035 pooled events)
(F) Half decay time kinetics for spontaneous quantal responses. Spontaneous quantal $\Delta F/F$ events were first averaged for each Ib or Is NMJ. The decay phase of these average traces was then fit to a double exponential curve to calculate the mean half decay time for each NMJ.
(G) Optical quantal $\Delta F/F$ responses at multiple Ca^{2+} concentrations in WT SynapGCaMP6f larvae. In all cases the Mg^{2+} concentration was 25 mM. Each data point represents the average of the NMJ mean optical quantal amplitude. The mean amplitude at each concentration was then fit with a linear regression with the indicated slopes and R^2 values (Pearson's tests Ib: r = 0.982, p = 0.003 and Is: r = 0.936, p = 0.02). (0.375 mM Ca^{2+} Ib n=7 NMJs, 847 events; 0.375 mM Ca^{2+} Is n=7 NMJs, 126 events; 0.75 mM Ca^{2+} Ib n=6 NMJs, 1714 events; 0.75 mM Ca^{2+} Is n=6 NMJs, 364 events; 1.0 mM Ca^{2+} Ib n=9 NMJs, 3318 events; 1.0 mM Ca^{2+} Is n=9 NMJs, 445 events; 1.5 mM Ca^{2+} Ib n=7 NMJs, 2729 events; 1.5 mM Ca^{2+} Is n=7 NMJs, 250 events; 2.0 mM Ca^{2+} Ib n=4 NMJs, 1645 events; 2.0 mM Ca^{2+} Is n=4 NMJs, 155 events)
(H-I) Thapsigargin has no effect on spontaneous optical quantal $\Delta F/F$ amplitudes. Animals were treated with 2 μM thapsigargin (or 0.2 % ethanol for the vehicle control) for 10 min with the brain intact to allow for muscle contractions in the presence of thapsigargin. Spontaneous events were recorded following removal of the brain in the continued presence of thapsigargin. (H) Cumulative probability for all Ib pooled spontaneous event maximum amplitudes (EtOH Ib: n = 6 NMJs, 1848 pooled events; thapsigargin Ib n = 12 NMJs, 3243 pooled events). (I) Cumulative probability for all Is pooled spontaneous event maximum amplitudes (EtOH Is: n = 6 NMJs, 205 pooled events; thapsigargin Is n = 12 NMJs, 509 pooled events). Insets show the mean (± SEM) spontaneous quantal $\Delta F/F$ time course for all pooled events.
(J-M) Simultaneous two-electrode voltage clamp and SynapGCaMP6f imaging shows that SynapGCaMP6f does not respond to membrane depolarization alone. (J) Representative example of the voltage clamp and imaging. Top trace (gray) shows the command voltage for the voltage clamp. 100 ms steps to the indicated voltages were then repeated at 2 s intervals before the axon was stimulated to produce evoked release. Motor neuron (MN) stimulation is indicated (red). Below the voltage is the current (black, I_m) during the whole recording showing the responses to the voltage steps and the EPSCs. The bottom four traces (green) are individual Ib synapse mean $\Delta F/F$ profiles that have been aligned to the voltage clamp recording. Spontaneous events are not time-locked to the motor neuron stimulation. (K) Higher resolution view of a spontaneous mEPSC example and the corresponding $\Delta F/F$ response (indicated in J, cyan box). (L) Higher resolution view of a depolarization, the corresponding current, and the fluorescence response at each synapse (indicated in J, blue box). (M) Higher resolution view of an EPSC and a corresponding quantal $\Delta F/F$ response (indicated in J, magenta box).
(N) NMJ area normalized spontaneous frequencies. Areas calculated using the total imaged Ib and Is SynapGCaMP6f baseline fluorescence regions. (Ib n = 9 NMJs; Is n = 9 NMJs; 9 NMJ pairs)
(O) Mean NMJ local spontaneous release frequencies. (Ib n = 9 NMJs; Is n = 9 NMJs; 9 NMJ pairs)
(P) Pooled cumulative probability distributions for the local spontaneous frequencies. (Ib n = 1070 spontaneously active sites; Is = 525 sites)
(Q) Spontaneously active site densities. Sites include all locations where there was at least one spontaneous event. Areas calculated as in (E). (Ib n = 9 NMJs; Is n = 9 NMJs; 9 NMJ pairs)
(R-S) Example of *post hoc* staining for Hrp and Brp following live SynapGCaMP6f imaging, specifically the example presented in Figures 3A-3E. (R) Maximum intensity projection for Hrp (green) and Brp (magenta) with Ib (blue) and Is (orange) axon borders indicated. (S) Isolated maximum intensity projection for Brp staining with Ib (blue) and Is (orange) axon borders.

(T) Mean Brp puncta density by NMJ. Areas were calculated using the corresponding Hrp motor neuron area. (Ib n = 21 NMJs; Is n = 20 NMJs; 18 NMJ pairs)
(U) Mean Brp puncta maximal intensity by NMJ. (Ib n = 21 NMJs; Is n = 20 NMJs; 18 NMJ pairs)
(V) Pooled cumulative probability distributions for the maximal intensity of all Brp puncta. (Ib n = 3461 puncta; Is n = 1609 puncta).
(W) Ratio of spontaneously active sites to Brp puncta within the corresponding NMJ and MN areas. (Ib n = 7 NMJs; Is n = 7 NMJs; 7 NMJ pairs)
Mean ± SEM indicated in relevant panels. Comparisons made with Pearsons's test (D, G), Student's t-test (A, F, N, O, Q, T, U, W), Kolmogorov-Smirnov test (D, P, V), or Kruskal-Wallis with Tukey's *post hoc* test (H, I). ** $p < 0.01$, *** $p < 0.001$, **** $p < 0.0001$ or NS not significant.

Figure S4

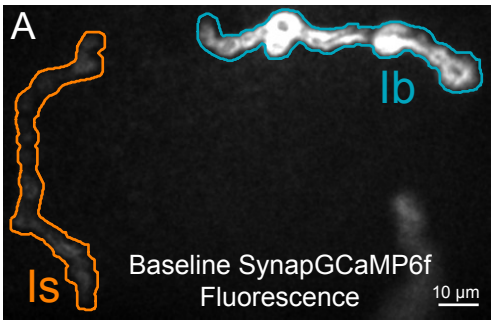
A
Ib
Is
Baseline SynapGCaMP6f
Fluorescence
10 µm

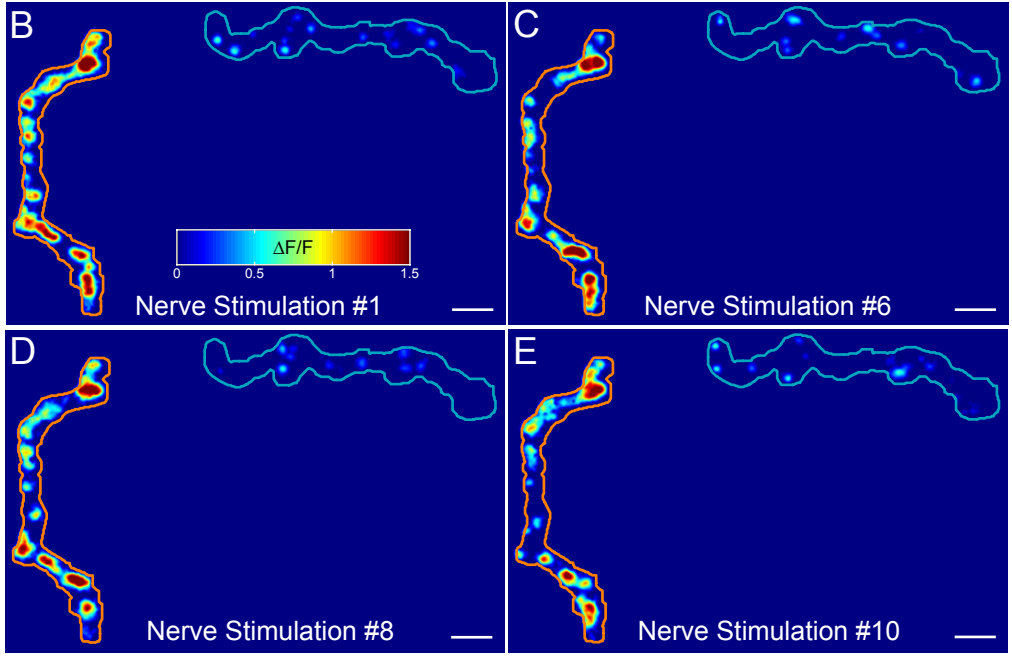
B
ΔF/F
0
0.5
1
1.5
Nerve Stimulation #1
C
Nerve Stimulation #6
D
Nerve Stimulation #8
E
Nerve Stimulation #10

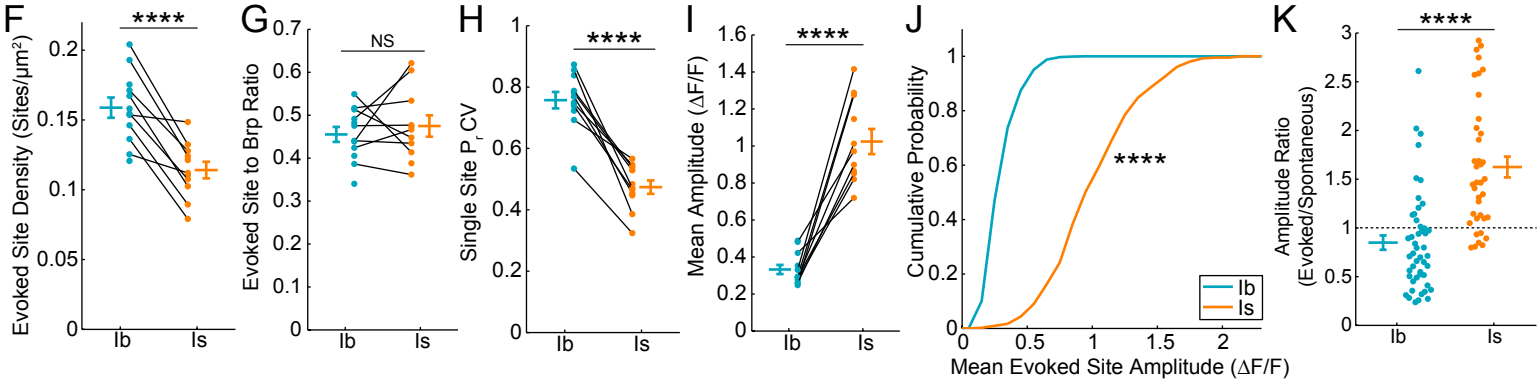
F
Evoked Site Density (Sites/µm²)
****
Ib
Is
G
Evoked Site to Brp Ratio
NS
H
Single Site Pr CV
****
I
Mean Amplitude (ΔF/F)
****
J
Cumulative Probability
****
Ib
Is
Mean Evoked Site Amplitude (ΔF/F)
K
Amplitude Ratio
(Evoked/Spontaneous)
****

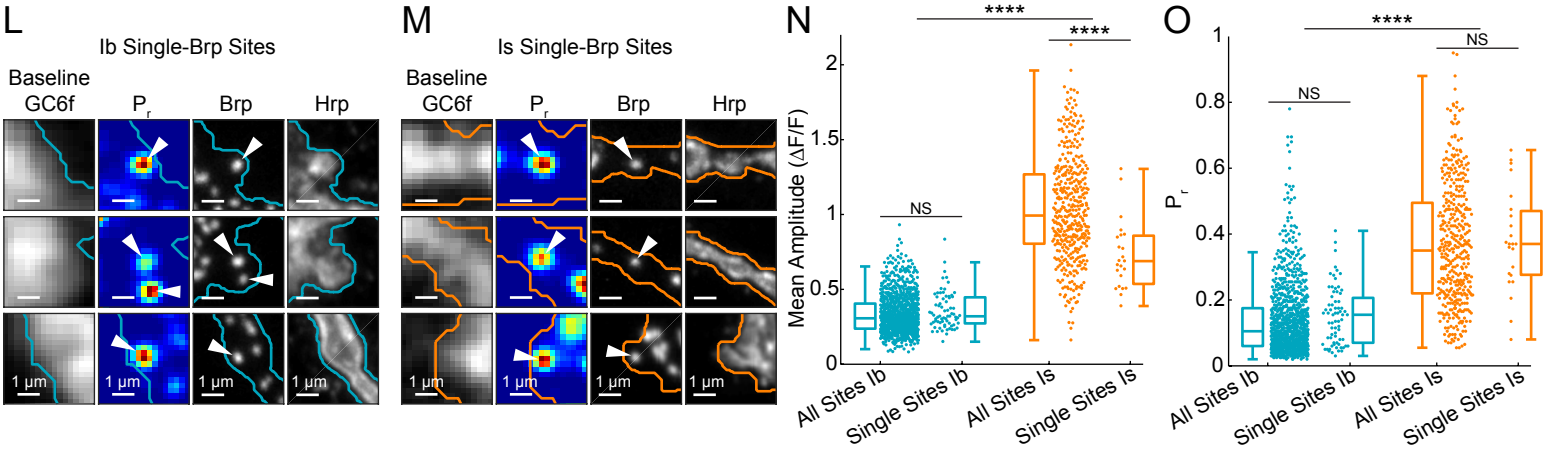
L
Ib Single-Brp Sites
Baseline
GC6f
Pr
Brp
Hrp
1 µm
M
Is Single-Brp Sites
N
Mean Amplitude (ΔF/F)
****
****
NS
All Sites Ib
Single Sites Ib
All Sites Is
Single Sites Is
O
Pr
****
NS
NS

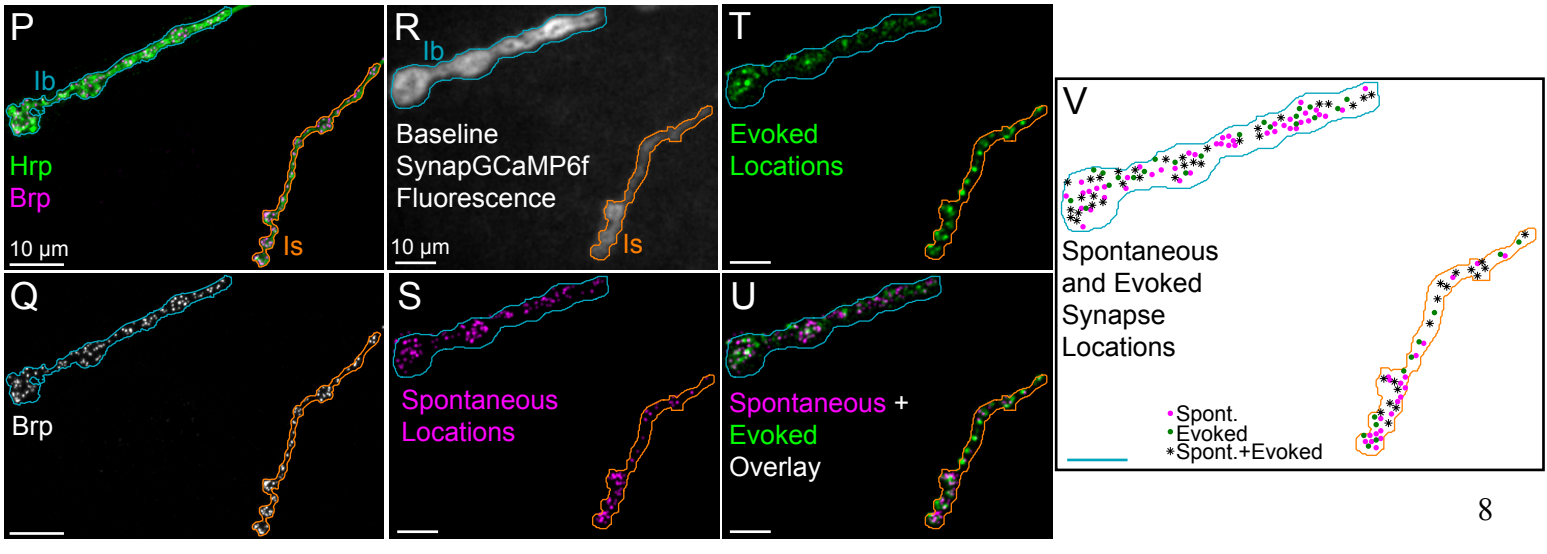
P
Ib
Hrp
Brp
10 µm
Is
R
Ib
Baseline
SynapGCaMP6f
Fluorescence
10 µm
Is
T
Evoked
Locations
V
Spontaneous
and Evoked
Synapse
Locations
Spont.
Evoked
Spont.+Evoked
Q
Brp
S
Spontaneous
Locations
U
Spontaneous +
Evoked
Overlay

Figure S4. Additional characterization of wild-type Ib and Is low frequency evoked activity (Related to Figure 4)

(A) Baseline SynapGCaMP6f fluorescence with Ib (blue) and Is (orange) NMJ borders highlighted. Example is the same as in Figure 4.

(B-E) Examples of identified quantal $\Delta F/F$ locations for individual APs in Ib (blue) and Is (orange) NMJs. Examples correspond to single trials in the recording presented in **Supplemental Movie 6** as well as the map presented in Figure 4.

(F) Mean MN-evoked active site density by NMJ. Active sites were defined as any isolatable active site used for the single-synapse P_r calculations. Areas were calculated using the area corresponding to the analyzed baseline SynapGCaMP6f fluorescence region. (Ib n = 12 NMJs; Is n = 11 NMJs; 9 NMJ pairs)

(G) Ratio of evoked sites to Brp puncta within the corresponding NMJ and MN areas. (Ib n = 12 NMJs; Is n = 11 NMJs; 9 NMJ pairs)

(H) Coefficient of variation for individual NMJ single-site P_r distributions. (Ib n = 12 NMJs; Is n = 11 NMJs; 9 NMJ pairs)

(I) Mean evoked site response amplitudes ($\Delta F/F$) by NMJ for low frequency stimulation (200 trials 0.1 Hz; Ib n = 12 NMJs; Is n = 11 NMJs; 9 NMJ pairs).

(J) Pooled cumulative probability distributions for all mean evoked release site amplitudes ($\Delta F/F$; 200 trials 0.1 Hz; Ib n = 995 sites; Is n = 413 sites).

(K) Spontaneous versus evoked release response amplitude ($\Delta F/F$) ratio during simultaneous recordings. Spontaneous quantal responses were recorded simultaneously during 100s seconds of continuous imaging during which 10 stimuli were also delivered at 0.1 Hz. Quantal responses were identified using the exact same detection settings and separated by their timing relative to the MN stimulation. Only synapses that had at least one spontaneous and one evoked event were included in the analysis. Ratios were calculated using the average response amplitudes for either evoked or spontaneous transmission at each of these sites (Ib n = 5 NMJs with n = 48 sites; Is n = 5 NMJs n = 38 sites).

(L and M) Examples of single-Brp evoked sites at Ib NMJs (L) and Is NMJs (M). Showing the baseline SynapGCaMP6f (GC6f) fluorescence (far left), probability map (middle left), Brp (middle right), and Hrp (far right) along with the analysis borders. All evoked sites used for the analysis (N and O) had an unambiguous and well-isolated Brp punctum in the corresponding *post hoc* antibody labeled image indicated with an arrowhead in these examples.

(N) Comparison of all pooled Ib and Is mean evoked release site amplitudes ($\Delta F/F$) with the subset of single-Brp evoked sites and the corresponding box plots to indicate the median and distribution of the respective populations ($\Delta F/F$; Ib n = 995 sites total with n = 71 single-Brp sites; Is n = 413 sites total with n = 23 single-Brp sites).

(O) Comparison of all pooled Ib and Is evoked release site P_r values along with the subset of single-Brp evoked sites and the corresponding box plots to indicate the median and distribution of the respective populations (Ib n = 995 sites total with n = 71 single-Brp sites; Is n = 413 sites total with n = 23 single-Brp sites).

(P) Maximum intensity projection for Hrp (green) and Brp (magenta) with Ib (blue) and Is (orange) axon borders.

(Q) Isolated maximum intensity projection for Brp staining with Ib (blue) and Is (orange) axon borders.

(R) Baseline SynapGCaMP6f fluorescence with Ib (blue) and Is (orange) NMJ borders highlighted.

(S) Cumulative spontaneous quantal release location heatmap (120s continuous imaging; magenta)

(T) Cumulative AP-evoked quantal release location heatmap (200 trials at 0.1 Hz; green). Recording of evoked release occurred after analysis of spontaneous release in (U).

(U) Merged image showing spontaneous (magenta) and evoked (green) release locations. White regions indicate areas participating in both forms of glutamate release. 2D cross-correlations were performed on the spontaneous versus evoked images to calculate the degree of overlap (see main text).

(V) Locations of all spontaneously active synapses (magenta dots, any isolated site with at least one spontaneous event), all evoked active synapses (green dots, any site that participated at least 3 times during 200 stimulus trials), and dual sites (*) where spontaneous and evoked synapses were located within less than 1 pixel (approx. 0.25 μm) of one another.

Comparisons made with Student's t-test (F, G, H, I), Kolmogorov-Smirnov test (J, K), or Kruskal-Wallis with Tukey's *post hoc* test (N, O). **** $p < 0.0001$ or NS not significant.

Figure S5

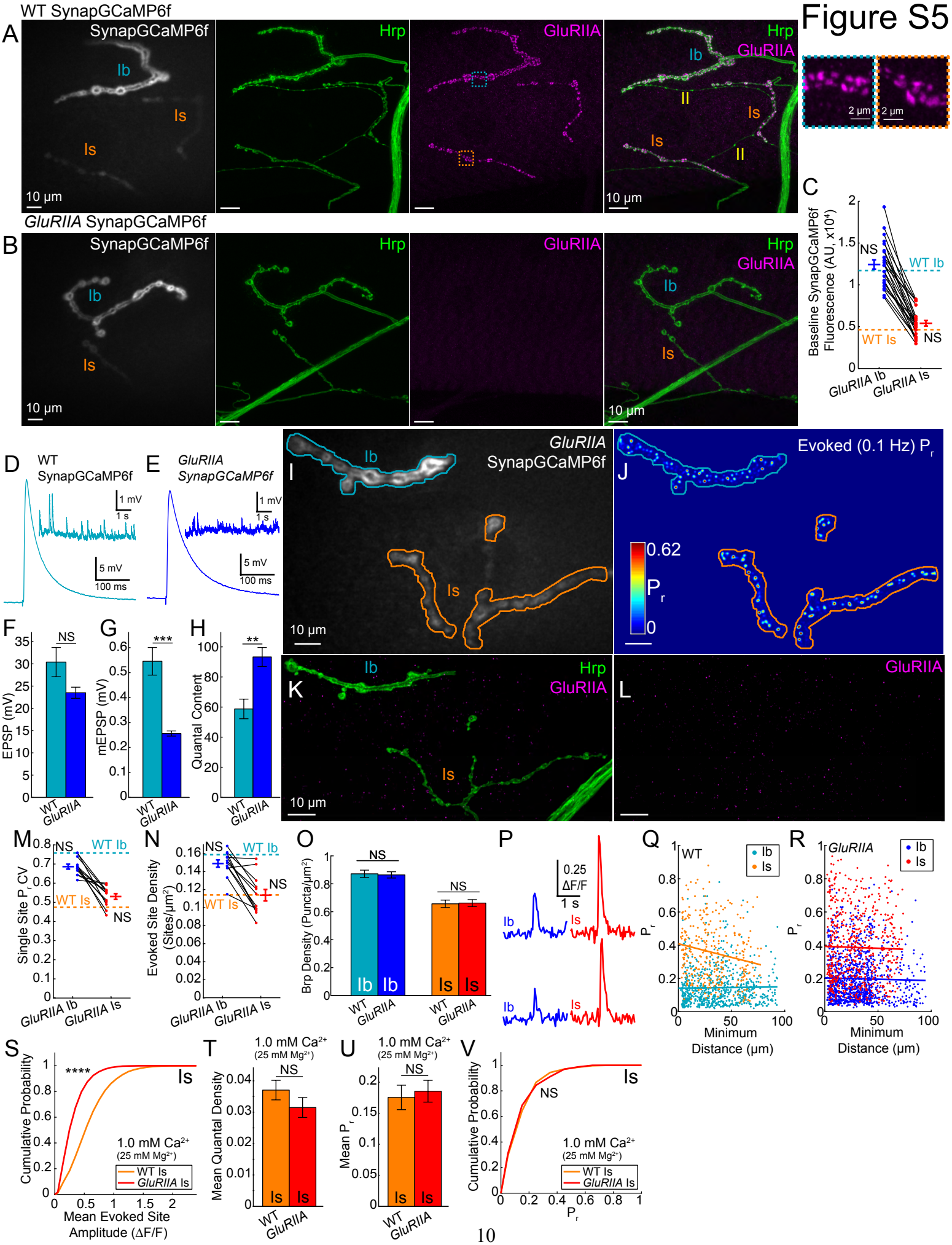
WT SynapGCaMP6f
A
SynapGCaMP6f
Ib
Is
Is
10 µm
Hrp
GluRIIA
Hrp
GluRIIA
Ib
II
Is
Is
II
10 µm
2 µm
2 µm
GluRIIA SynapGCaMP6f
B
SynapGCaMP6f
Ib
Is
10 µm
Hrp
GluRIIA
Hrp
GluRIIA
Ib
Is
10 µm
C
Baseline SynapGCaMP6f Fluorescence (AU, x10⁴)
NS
WT Ib
WT Is
NS
GluRIIA Ib
GluRIIA Is
D
WT SynapGCaMP6f
1 mV
1 s
5 mV
100 ms
E
GluRIIA SynapGCaMP6f
1 mV
1 s
5 mV
100 ms
I
GluRIIA SynapGCaMP6f
Ib
Is
10 µm
J
Evoked (0.1 Hz) Pr
0.62
Pr
0
K
Ib
Hrp
GluRIIA
Is
10 µm
L
GluRIIA
F
EPSP (mV)
NS
WT
GluRIIA
G
mEPSP (mV)
***
WT
GluRIIA
H
Quantal Content
**
WT
GluRIIA
M
Single Site Pr CV
NS
WT Ib
WT Is
NS
GluRIIA Ib
GluRIIA Is
N
Evoked Site Density (Sites/µm²)
NS
WT Ib
WT Is
NS
GluRIIA Ib
GluRIIA Is
O
Brp Density (Puncta/µm²)
NS
NS
Ib
Ib
Is
Is
WT
GluRIIA
WT
GluRIIA
P
0.25
ΔF/F
1 s
Ib
Is
Ib
Is
Q
WT
Ib
Is
Pr
Minimum Distance (µm)
R
GluRIIA
Ib
Is
Pr
Minimum Distance (µm)
S
Cumulative Probability
****
Is
1.0 mM Ca2+
(25 mM Mg2+)
WT Is
GluRIIA Is
Mean Evoked Site Amplitude (ΔF/F)
T
1.0 mM Ca2+
(25 mM Mg2+)
Mean Quantal Density
NS
Is
Is
WT
GluRIIA
U
1.0 mM Ca2+
(25 mM Mg2+)
Mean Pr
NS
Is
Is
WT
GluRIIA
V
Cumulative Probability
NS
Is
1.0 mM Ca2+
(25 mM Mg2+)
WT Is
GluRIIA Is
Pr

Figure S5. Additional characterization of *GluRIIA* properties (Related to Figure 5)

(A-B) Baseline SynapGCaMP6f fluorescence along with maximum intensity for Hrp (green), GluRIIA (magenta), and the merged image for WT SynapGCaMP6f (A) and *GluRIIA* SynapGCaMP6f (B) animals. Type II axons (yellow) are also indicated but are not labeled with either SynapGCaMP6f or the GluRIIA antibody (A). Insets to right in (A) show a higher resolution view of the GluRIIA clusters at Ib (blue) and Is (orange) NMJs.

(C) *GluRIIA* SynapGCaMP6f mean baseline SynapGCaMP6f fluorescence. (*GluRIIA* Ib n = 24 NMJs; *GluRIIA* Is n = 24 NMJs; 24 NMJ pairs)

(D-H) Electrophysiological analysis shows normal homeostatic compensation of the compound quantal content in the presence of SynapGCaMP6f. (D) Representative individual EPSPs in a WT SynapGCaMP6f larva with the inset being a representative trace showing mEPSPs. (E) Representative individual EPSP in a *GluRIIA* SynapGCaMP6f larva with the inset being a representative trace showing mEPSPs. (F) Mean EPSP amplitude for WT SynapGCaMP6f and *GluRIIA* SynapGCaMP6f NMJs. (G) Mean mEPSP amplitude for multiple NMJs. (H) Mean quantal content for each NMJ. Calculated as the mean EPSP/mEPSP amplitude for each NMJ. All measurements were performed in segment A3 (WT n = 11 NMJs; *GluRIIA* n = 10 NMJs)

(I-L) Example of optical quantal analysis on a *GluRIIA* SynapGCaMP6f muscle 4 NMJ including the baseline SynapGCaMP6f fluorescence (I) with Ib (blue) and Is (orange) NMJ borders highlighted, cumulative AP-evoked quantal release location heatmap (J) (200 trials at 0.1 Hz; green), as well as the corresponding maximum intensity projection for Hrp (green) and GluRIIA (magenta) (K) and the maximum intensity projection for GluRIIA alone (magenta) confirming the *GluRIIA* genotype (L).

(M) *GluRIIA* SynapGCaMP6f coefficient of variation for individual NMJ P_r distributions. (Ib n = 12 NMJs; Is n = 12 NMJs; 12 NMJ pairs).

(N) *GluRIIA* SynapGCaMP6f mean MN-evoked active site density by NMJ. Active sites were defined as described previously (see Figure S4F) (Ib n = 12 NMJs; Is n = 12 NMJs; 12 NMJ pairs).

(O) Mean Brp puncta density by NMJ. Areas were calculated using the corresponding Hrp motor neuron area. (WT Ib n = 16 NMJs and WT Is n = 16 NMJs from 5 larvae; *GluRIIA* Ib n = 17 NMJs and *GluRIIA* Is n = 17 NMJs from 5 larvae).

(P) Mean single synapse $\Delta F/F$ traces for examples of single spontaneous release events at *GluRIIA* Ib (blue) and *GluRIIA* Is (red) NMJs showing the relationship between the signal and the background noise.

(Q-R) Comparison between the mean evoked P_r at each synapse and the minimum distance to the nearest neighboring synapse in the corresponding axon for both WT SynapGCaMP6f (Q) and *GluRIIA* SynapGCaMP6f (R). Linear regressions are indicated (WT Ib r = 0.017, NS; WT Is r = -0.19, ***; *GluRIIA* Ib r = -0.023, NS; *GluRIIA* Is r = -0.023, NS)

(S-V) Optical quantal analysis of Is NMJ evoked transmission properties in lower Ca^{2+} saline shows no presynaptic compensation (HL3 with 1.0 mM Ca^{2+}, 25 mM Mg^{2+}). Analysis of Ib transmission is not possible as the reduced Ca^{2+} concentration and *GluRIIA* mutation reduces the amplitude of the optical quantal events to our detection threshold. However, low Ca^{2+} *GluRIIA* responses at the Is NMJs are still detectable. (S) Pooled mean optical evoked amplitudes for WT Is and *GluRIIA* Is sites show a significant reduction in *GluRIIA* animals. (T) Mean quantal density for multiple NMJs shows no difference in the normalized quantal output of the Is NMJs in these genotypes. (U) Mean NMJ P_r shows no difference at Is synapses. In both cases P_r has been reduced to a level comparable to WT Ib P_r in 1.5 mM Ca^{2+} (see Figure 4L) (V) Cumulative probability for single synapse P_r at all pooled WT and *GluRIIA* Is synapses in low Ca^{2+} also shows no difference in synaptic strength. (1.0 mM Ca^{2+} WT n = 5 NMJs and 339 pooled sites; 1.0 mM Ca^{2+} *GluRIIA* n = 5 NMJs and 328 pooled sites)

In relevant plots (C, M, N), data for WT Ib (blue dashed line) or WT Is (orange dashed line) are presented for comparisons and correspond to the same mean data presented in Figure 4 and S4). Comparisons made with Pearsons's test (Q, R), Student's t-test (F, G, H, T, U), Kolmogorov-Smirnov test (S, V), one-way ANOVA with Tukey's *post hoc* test (C, M, N, O) or Pearson's test (L-M). * $p < 0.05$, ** $p < 0.01$, *** $p < 0.001$, **** $p < 0.001$ or NS not significant.

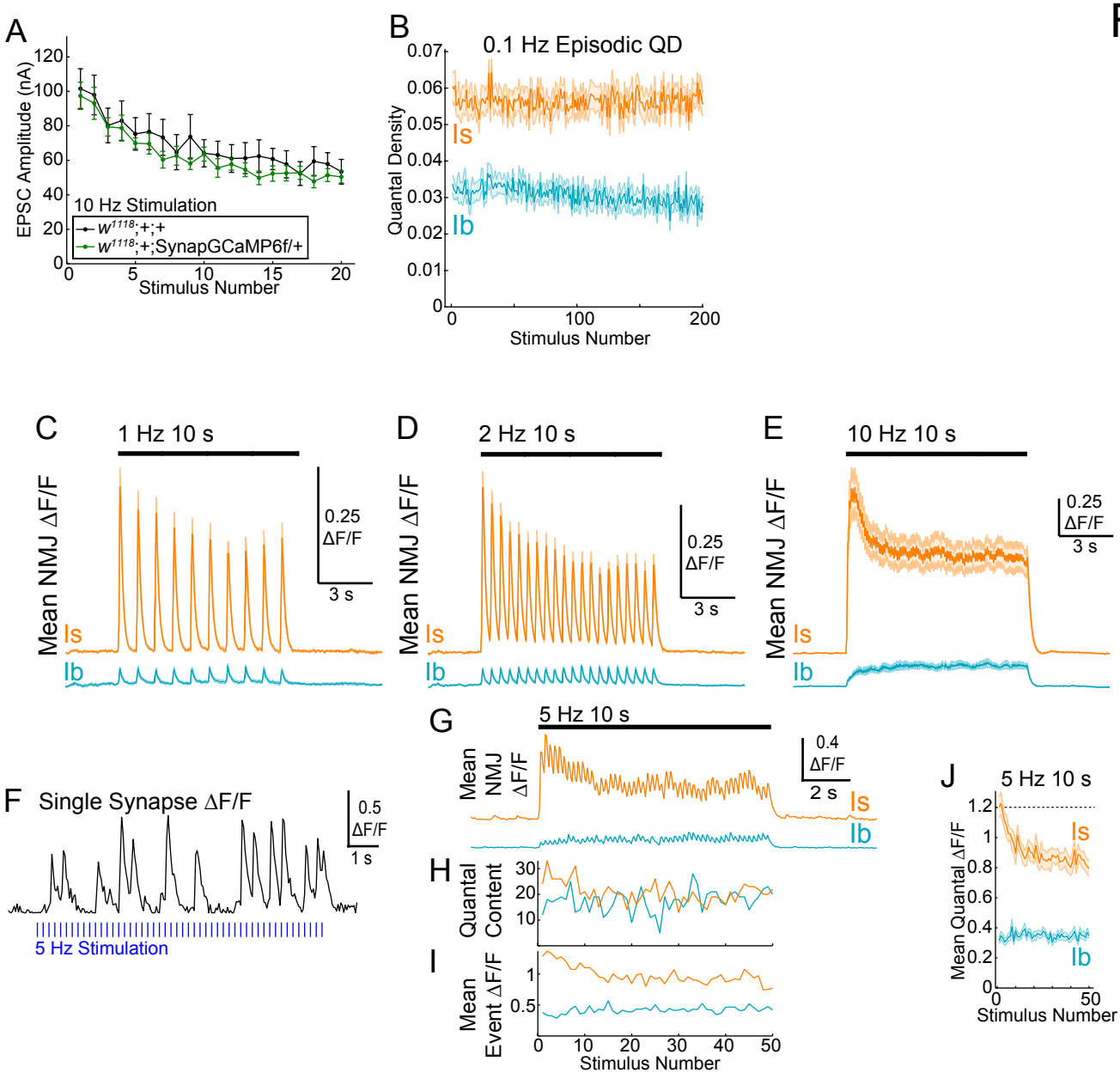
A
EPSC Amplitude (nA)
10 Hz Stimulation
w1118;+;+
w1118;+;SynapGCaMP6f/+
Stimulus Number
B
0.1 Hz Episodic QD
Quantal Density
Is
Ib
Stimulus Number
C
1 Hz 10 s
Mean NMJ ΔF/F
0.25 ΔF/F
3 s
Is
Ib
D
2 Hz 10 s
E
10 Hz 10 s
F
Single Synapse ΔF/F
0.5 ΔF/F
1 s
5 Hz Stimulation
G
5 Hz 10 s
Mean NMJ ΔF/F
0.4 ΔF/F
2 s
H
Quantal Content
I
Mean Event ΔF/F
Stimulus Number
J
5 Hz 10 s
Mean Quantal ΔF/F
Stimulus Number
K
Is
5 Hz Stimulus Activity Map
Total # Events
0
33
Ib
10 μm
L
5 Hz Stimulus Plasticity Map
Depressed/Silenced
Unchanged
Facililitated/Recruited
10 μm
M
% Active Pixels
Ib
Is
Depressed/ Silenced
Unchanged
Facililitated/ Recruited

Figure S6. Additional optical quantal analysis during different stimulation frequencies (Related to Figure 6)
(A) Short-term depression in compound EPSC amplitudes during a 10 Hz stimulation shows no difference with or without the expression of SynapGCaMP6f. (w^{1118};+;+ n = 4 NMJs; w^{1118}:+/+;SynapGCaMP6f/+ n = 5 NMJs)
(B) Quantal density versus stimulation trial during 0.1 Hz episodic stimulation shows stable responses for > 30 min (0.1 Hz Ib n = 12 NMJs; 0.1 Hz Is n = 11 NMJ)
(C-E) Mean NMJ $\Delta F/F$ traces for 10 s stimuli at (C) 1 Hz, (D) 2 Hz, and (E) 10 Hz. (1 Hz 10s Ib n = 11 NMJs; 1 Hz 10s Is n = 11 NMJs; 2 Hz 10s Ib n = 13 NMJs; 2 Hz 10s Is n = 13 NMJs; 10 Hz 10s Ib n = 7 NMJs; 10 Hz 10s Is n = 7 NMJs)
(F) An example of a single Ib synapse $\Delta F/F$ trace during a 5 Hz nerve stimulation. Quantal responses are relatively uniform in both size and kinetics, with individual peaks being identifiable during the stimulus period as they are able to decay before another vesicle is released. Blue hash marks indicate when action potentials were initiated.
(G-I) An example of high frequency optical quantal analysis corresponding to **Supplemental Movie 7**. (G) Mean $\Delta F/F$ for the whole imaged Ib and Is region during a 10s, 5 Hz stimulus. (H) Total quantal content per stimulus during the stimulus train. (I) The mean event amplitude per stimulus during the stimulus train.
(J) Mean quantal response amplitudes during 5 Hz stimulus. Data corresponds to the quantal response in Figure 6C and 6D. The declining amplitudes in the Is NMJs during this stimulus period are due to the decrease in quantal density reducing the overlap of quantal spots (See Methods for a more detailed explanation). No change in the amplitudes were noted at Ib NMJs. (Ib n = 13 and Is n = 13 NMJs).
(K) A quantal activity heatmap during a 5 Hz stimulus scaled to the total number of events at each synapse during the 50 stimulus trials. Ib (blue) and Is (orange) NMJ borders highlighted. Data corresponds to **Supplemental Movie 7** and (G-I),
(L-M) Single pixel quantal plasticity analysis during the same 5 Hz 10s stimulus example in (G-I and K), including the locations of pixels that were either depressed/silenced (red), unchanged (blue), or facilitated/recruited (green) and (M) the corresponding percent of active pixel breakdown of these categories for both the Ib and Is NMJ.
All lines for multiple NMJs (B-E and J) are mean ± SEM.

Figure S7

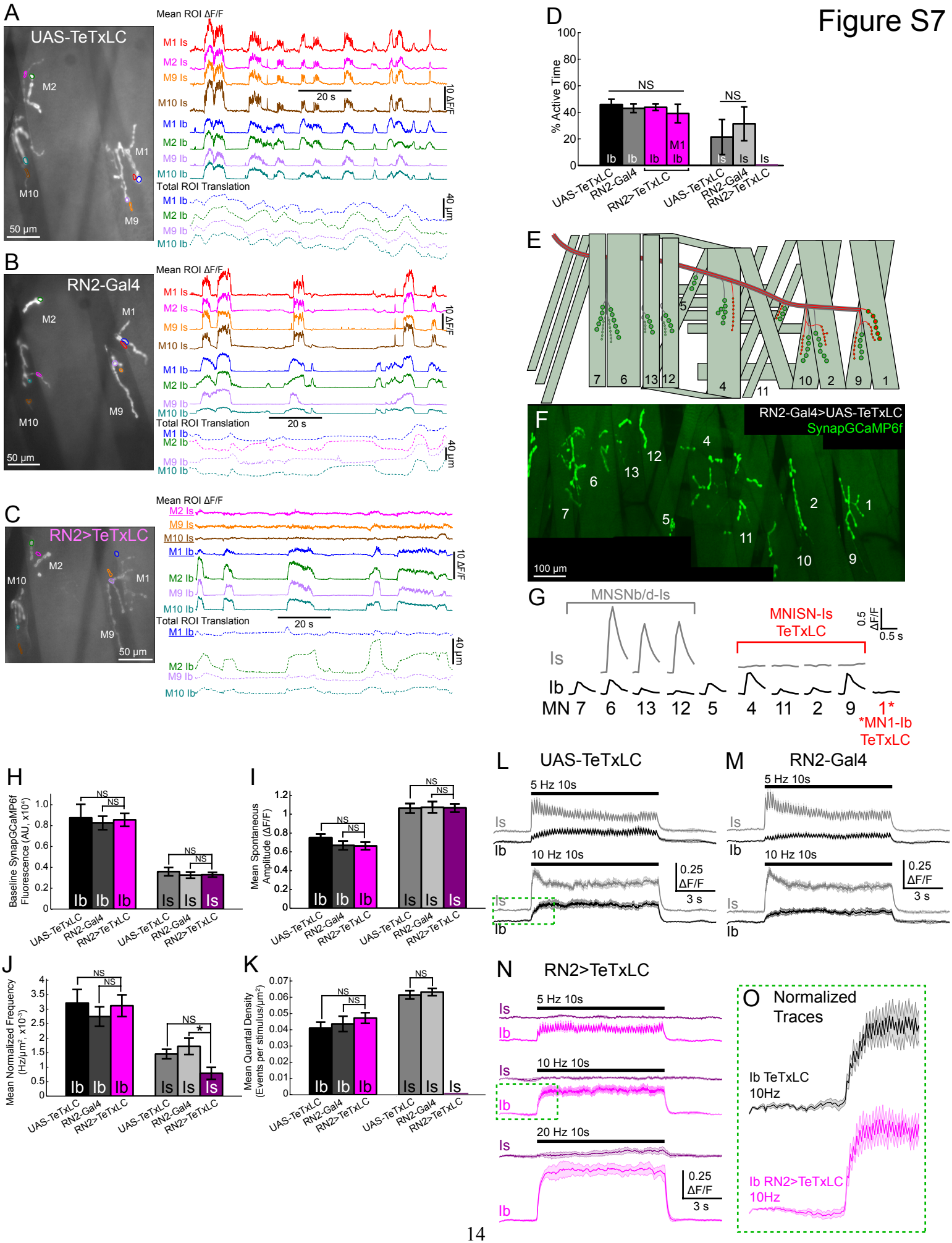
A
UAS-TeTxLC
M2
M1
M10
M9
50 µm
Mean ROI ΔF/F
M1 Is
M2 Is
M9 Is
M10 Is
20 s
10 ΔF/F
M1 Ib
M2 Ib
M9 Ib
M10 Ib
Total ROI Translation
40 µm
B
RN2-Gal4
C
RN2>TeTxLC
D
% Active Time
NS
Ib
Is
M1
E
F
RN2-Gal4>UAS-TeTxLC
SynapGCaMP6f
100 µm
G
MNSNb/d-Is
MNISN-Is
TeTxLC
0.5 ΔF/F
0.5 s
MN 7 6 13 12 5 4 11 2 9 1*
*MN1-Ib
TeTxLC
H
Baseline SynapGCaMP6f Fluorescence (AU, x10⁴)
UAS-TeTxLC
RN2-Gal4
RN2>TeTxLC
I
Mean Spontaneous Amplitude (ΔF/F)
J
Mean Normalized Frequency (Hz/µm², x10⁻³)
K
Mean Quantal Density (Events per stimulus/µm²)
L
UAS-TeTxLC
5 Hz 10s
10 Hz 10s
0.25 ΔF/F
3 s
M
RN2-Gal4
N
RN2>TeTxLC
20 Hz 10s
O
Normalized Traces
Ib TeTxLC 10Hz
Ib RN2>TeTxLC 10Hz

Figure S7. Additional characterization of TeTxLC expression experiments (Related to Figure 7)
(A-C) Additional breakdown of the three example recordings presented in Figure 7 and **Supplemental Movie 8**. Data includes a reference image with the single bouton ROIs highlighted (*left*), single bouton Δ*F*/*F* traces (*right top*) and single bouton total translation data (*right bottom*) for UAS-TeTxLC SynapGCaMP6f (A), RN2-Gal4 SynapGCaMP6f (B) and RN2-Gal4>UAS-TeTxLC SynapGCaMP6f (C).
(D) Quantification of the total percent active time at Ib and Is NMJs for UAS-TeTxLC SynapGCaMP6f larvae, RN2-Gal4 SynapGCaMP6f larvae, and RN2>TeTxLC SynapGCaMP6f larvae. Note that M1-Ib in the RN2>TeTxLC genotype was separated for this analysis because it also expresses TeTxLC and RN2>TeTxLC Is NMJs never showed any evidence of activity. (*n* = 8 larvae UAS-TeTxLC SynapGCaMP6f; *n* = 8 larvae RN2-Gal4 SynapGCaMP6f; *n* = 8 larvae RN2-Gal4>UAS-TeTxLC SynapGCaMP6f)
(E-G) TeTxLC expression under the control of the RN2-Gal4 selectively impairs evoked glutamate release from the MNISN-Is and MN1-Ib motor neurons. (E) Schematic showing a hemisegment with the expression pattern of RN2-Gal4 indicated in red. (F) Multiple stitched maximum intensity projections of corresponding to a single RN2-Gal4>UAS-TeTxLC SynapGCaMP6f hemisegment. Muscle numbers indicated. (G) Single-AP Δ*F*/*F* traces for single boutons during 0.1 Hz stimulation from the Ib and Is NMJs in (F). RN2-Gal4 expresses in MNISN-Is and MN1-Ib (both indicated in red). No responses were detected in the presence of TeTxLC. Data were acquired with a 20x water objective to collect responses at multiple neighboring NMJs simultaneously.
(H) Mean baseline SynapGCaMP6f fluorescence for UAS-TeTxLC SynapGCaMP6f (Ib *n* = 8 NMJs; Is *n* = 8 NMJs), RN2-Gal4 SynapGCaMP6f (Ib *n* = 6 NMJs; Is *n* = 6 NMJs), and RN2-Gal4>UAS-TeTxLC SynapGCaMP6f (Ib *n* = 7 NMJs; Is *n* = 7 NMJs)
(I) Mean spontaneous quantal event amplitudes (Δ*F*/*F*) by NMJ for UAS-TeTxLC SynapGCaMP6f (Ib *n* = 13 NMJs; Is *n* = 13 NMJs), RN2-Gal4 SynapGCaMP6f (Ib *n* = 12 NMJs; Is *n* = 12 NMJs), and RN2-Gal4>UAS-TeTxLC SynapGCaMP6f (Ib *n* = 16 NMJs; Is *n* = 16 NMJs)
(J) NMJ area normalized spontaneous frequencies. Areas calculated using the total imaged Ib and Is SynapGCaMP6f baseline fluorescence regions. Only a minor decrease in the rate of spontaneous release was noted at the TeTxLC-expressing Is NMJs.
(K) Mean quantal density during 0.1 Hz stimuli (200 trials) for UAS-TeTxLC SynapGCaMP6f (Ib *n* = 8 NMJs; Is *n* = 8 NMJs), RN2-Gal4 SynapGCaMP6f (Ib *n* = 6 NMJs; Is *n* = 6 NMJs), and RN2-Gal4>UAS-TeTxLC SynapGCaMP6f (Ib *n* = 7 NMJs; Is *n* = 7 NMJs)
(L-O) High frequency stimulus Δ*F*/*F* analysis. (L) UAS-TeTxLC SynapGCaMP6f 10s, 5 Hz stimulus (*Top,* Ib *n* = 4 NMJs; Is *n* = 4 NMJs) or 10s, 10 Hz stimulus (*Bottom,* Ib *n* = 4 NMJs; Is *n* = 4 NMJs). (M) RN2-Gal4 SynapGCaMP6f 10s, 5 Hz stimulus (*Top,* Ib *n* = 5 NMJs; Is *n* = 5 NMJs) or 10s, 10 Hz stimulus (*Bottom,* Ib *n* = 4 NMJs; Is *n* = 4 NMJs). (N) RN2-Gal4>UAS-TeTxLC SynapGCaMP6f 10s, 5 Hz stimulus (*Top,* Ib *n* = 4 NMJs; Is *n* = 4 NMJs) or 10s, 10 Hz stimulus (*Middle,* Ib *n* = 5 NMJs; Is *n* = 5 NMJs) or 10s, 20 Hz stimulus (*Bottom,* Ib *n* = 5 NMJs; Is *n* = 5 NMJs). Note that due to the large Is depolarization normally present during simultaneous stimulation of both axons, it is difficult to image during stimulation frequencies >15 Hz in control animals because of the large contractions that normally occur. However, in the absence of synchronous evoked Is release in these animals the muscles often fail to contract allowing for imaging at higher frequencies. Additionally, a small amount of glutamate release was noted at Is synapses often late during 20 Hz stimulation frequencies. However, the release never appeared to be synchronous among a large percentage of synapses along the Is axon expressing TeTxLC. (O) A higher resolution view of the Ib mean Δ*F*/*F* traces during the initial period of a 10 Hz stimulation (green dashed boxes in L and M) showing that both have similar activity at the stimulus onset.

Figure S8

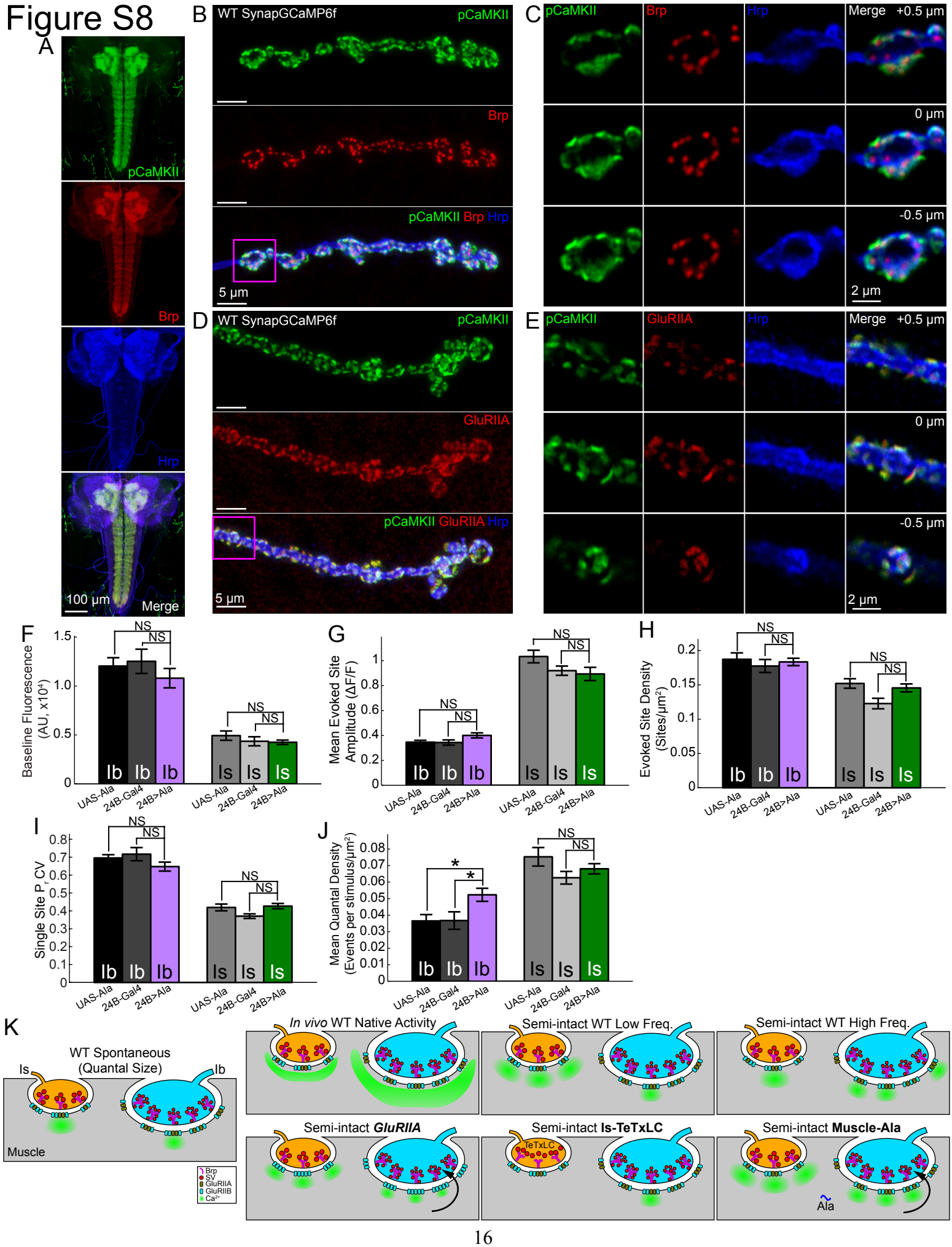
A
pCaMKII
Brp
Hrp
100 µm
Merge
B
WT SynapGCaMP6f
pCaMKII
Brp
pCaMKII Brp Hrp
5 µm
C
pCaMKII
Brp
Hrp
Merge +0.5 µm
0 µm
-0.5 µm
2 µm
D
WT SynapGCaMP6f
pCaMKII
GluRIIA
pCaMKII GluRIIA Hrp
5 µm
E
pCaMKII
GluRIIA
Hrp
Merge +0.5 µm
0 µm
-0.5 µm
2 µm
F
Baseline Fluorescence (AU, x10⁴)
G
Mean Evoked Site Amplitude (ΔF/F)
H
Evoked Site Density (Sites/µm²)
I
Single Site P_r CV
J
Mean Quantal Density (Events per stimulus/µm²)
NS
*
Ib
Is
UAS-Ala
24B-Gal4
24B>Ala
K
WT Spontaneous (Quantal Size)
Is
Ib
Muscle
In vivo WT Native Activity
Semi-intact WT Low Freq.
Semi-intact WT High Freq.
Semi-intact GluRIIA
Semi-intact Is-TeTxLC
TeTxLC
Semi-intact Muscle-Ala
Ala
Brp
SV
GluRIIA
GluRIIB
Ca²⁺

Figure S8. Additional characterization of postsynaptic CaMKII inhibition experiments (Related to Figure 8)
(A) A maximum intensity projection of the WT SynapGCaMP6f larval central nervous system that has been labeled with pCaMKII, Brp, and Hrp antibodies. Note that this pCaMKII antibody clearly labels the neuropil as seen through approximate overlap with Brp.
(B-C) pCaMKII and Brp show little colocalization at individual synapses in Ib boutons from a WT SynapGCaMP6f larva. (B) A high-resolution representative Ib NMJ maximum intensity projection labeled with pCaMKII, Brp, and Hrp antibodies showing that pCaMKII and Brp do not colocalize. Magenta box identifies the bouton in (C). (C) Individual confocal slices through a 1 μm section of a single bouton.
(D-E) pCaMKII and GluRIIA show a high degree of colocalization at individual synapses in Ib boutons from a WT SynapGCaMP6f larva. (B) A high-resolution representative Ib NMJ (see Figure 8A) maximum intensity projection labeled with pCaMKII, GluRIIA, and Hrp antibodies showing that pCaMKII and Brp do not colocalize. Magenta box identifies the bouton in (E). (E) Individual confocal slices through a 1 μm section of a single bouton.
(F-J) Additional analysis of Ala expression in the muscle and relevant controls including, mean baseline SynapGCaMP6f fluorescence (F), mean evoked amplitudes by NMJ during 0.1 Hz stimuli (200 trials) (G), mean evoked site density (H), the coefficient of variation for the individual NMJ P_r distributions (I), and mean quantal densities (J). Genotypes included UAS-Ala SynapGCaMP6f (Ib n = 8 NMJs; Is n = 8 NMJs), 24B-Gal4 SynapGCaMP6f (Ib n = 8 NMJs; Is n = 8 NMJs), and 24B-Gal4>UAS-Ala SynapGCaMP6f (Ib n = 9 NMJs; Is n = 9 NMJs)
(K) Summary model of results. Ib NMJs have larger boutons with more synapses and smaller quantal sizes. *In vivo* Ib NMJs have significantly higher total integrated postsynaptic Ca^{2+} activity during MN activity. Under basal conditions Is NMJs release more glutamate, however during stimulation of the motor neuron at high frequencies Is release is depressed, while Ib release is facilitated by recruiting silent sites. In *GluRIIA* larvae, quantal sizes are reduced at both NMJs but presynaptic release is only increased at Ib synapses via a retrograde signal. Silencing of evoked transmitter release from the Is NMJ with TeTxLC has no effect on Ib release, however postsynaptic inhibition of CaMKII with the Ala peptide produces a selective retrograde enhancement of Ib release.
Comparisons made with one-way ANOVA with Tukey's *post hoc* test (F-J). * $p < 0.05$, **** $p < 0.001$ or NS not significant.

Supplemental Movie 1. *In vivo* SynapGCaMP6f imaging at low magnification (Related to Figure 1)
Example of low magnification multi-segment activity during a representative wave of activity in a SynapGCaMP6f expressing larva. Data were acquired at 40X magnification with an imaging frequency of 14 Hz and the movie playback is at 10 FPS. Scalebar is 1 mm. Data corresponds to the example in Figures 1C-D.

Supplemental Movie 2. *In vivo* SynapGCaMP6f imaging at high magnification with ROI tracking and activity traces (Related to Figure 1)
Example *in vivo* NMJ activity at four dorsal muscle cells during repeating endogenous activity bouts. Raw data on left was acquired at 260X magnification with an imaging frequency of 14 Hz and the movie playback is at 30 FPS. Scale bar is 50 μm. The ROI locations were determined by the image registration corrections and then applied to the raw data to calculate local SynapGCaMP6f activity. The corresponding $\Delta F/F$ traces are presented on the right, synchronized with the movie playback. All traces are on the same scale indicated in the upper right. Data corresponds to the example in Figures 1F-G and S1B.

Supplemental Movie 3. *In vivo* SynapGCaMP6f imaging can detect spontaneous quantal events at both Ib and Is NMJs (Related to Figure 2)
Example of the *in vivo* automatic detection of spontaneous quantal transmission. Analysis of spontaneous release was performed between motor neuron activity bouts. Raw data on the top was acquired with an imaging frequency of 14 Hz and movie playback is at 20 FPS. Scale bar is 10 μm. The locations of identified and validated spontaneous release events are indicated with a green circle that appears right before, during, and after the peak of the quantal response. The bottom movie is an overlay of the $\Delta F/F$ signal for the identified spontaneous quantal events on the basal SynapGCaMP6f fluorescence at each frame. Data corresponds to the example in Figures 2I-K and S2.

Supplemental Movie 4. SynapGCaMP6f imaging detects spontaneous quantal responses at both Ib and Is NMJs in the semi-intact larva (Related to Figure 3)
Example analysis of spontaneous optical quantal transmission in the semi-dissected larval fillet during confocal imaging. Data were acquired with an imaging frequency of 20 Hz and movie playback is at 20 FPS. The top movie is an overlay of the $\Delta F/F$ data on the basal SynapGCaMP6f fluorescence for the first frame with Ib (blue) and Is (orange) NMJ borders highlighted. Scale bar is 10 μm. Colorbar corresponds to the $\Delta F/F$. The bottom movie shows a cumulative map of all of the identified spontaneous quantal events as they occur in the top movie. Centroid locations are presented and added locally to give the local total counts. Note that the colorbar scale changes as some sites have more than one spontaneous transmission event. Data corresponds to the example in Figures 3A-E, 3L and S3R-S.

Supplemental Movie 5. SynapGCaMP6f spontaneous quantal responses compared to simultaneous electrophysiology at both Ib and Is NMJs in the semi-intact larva (Related to Figure 3)
Example analysis of simultaneous spontaneous optical quantal transmission with electrophysiology in the semi-dissected larval fillet during confocal imaging. Data were acquired with an imaging frequency of 20 Hz and movie playback is at 10 FPS. The top movie is an overlay of the $\Delta F/F$ data on the basal SynapGCaMP6f fluorescence for the first frame with Ib (blue) and Is (orange) NMJ borders highlighted. Scale bar is 10 μm. Colorbar corresponds to the $\Delta F/F$. The bottom movie shows the aligned voltage (V_m) measurement with mEPSPs as well as the mean single synapse $\Delta F/F$ traces for the identified optical quantal events. $\Delta F/F$ events are colored by their NMJ source (Ib, blue; Is, orange), as determined by the imaging data (top). Scale bars are indicated in red for both the V_m and the corresponding $\Delta F/F$ data. Note that not all mEPSPs have a corresponding optical event as we are not imaging the entire NMJ area for both Ib or Is inputs. Data corresponds to the example in Figures 3H and S3B-C.

Supplemental Movie 6. Optical quantal analysis using SynapGCaMP6f imaging detects synchronous MN-evoked quantal responses at both Ib and Is NMJs in the semi-intact larva (Related to Figure 4)
Example analysis of low frequency optical quantal analysis in the semi-dissected larval fillet during confocal imaging and 0.1 Hz nerve stimulation for 10 stimuli episodes. Data were acquired with an imaging frequency of 20 Hz and movie playback is at 10 FPS. The top movie is an overlay of the $\Delta F/F$ data on the basal SynapGCaMP6f fluorescence for the first frame with Ib (blue) and Is (orange) NMJ borders highlighted. Scale bar is 10 μm. Stimuli are noted with * in the upper right corner. Colorbar corresponds to the $\Delta F/F$. The bottom movie shows a cumulative map of all of the identified evoked quantal event locations as they occur in the top movie. Centroid locations are

presented and added locally to give the local total counts. Note that the colorbar scale changes as individual sites accumulate more evoked transmission events. Data corresponds to the example in Figures 4A-F and S4A-E.

Supplemental Movie 7. High frequency stimulation optical quantal analysis using SynapGCaMP6f imaging allows quantal responses to be separated during short high frequency nerve stimulation (5 Hz 10s). (Related to Figure 6)
Example analysis of high frequency optical quantal analysis in the semi-dissected larval fillet during confocal imaging and 5 Hz nerve stimulation for 10 s with continuous imaging. Data were acquired with an imaging frequency of 20 Hz and movie playback is at 20 FPS. The top left movie is an overlay of the $\Delta F/F$ data on the basal SynapGCaMP6f fluorescence for the first frame with Ib (blue) and Is (orange) NMJ borders highlighted. Scale bar is 10 μm. Stimuli are noted with * in the upper right corner. Colorbar corresponds to the $\Delta F/F$. The top right traces show the average $\Delta F/F$ data for the entire Ib (blue) or Is (orange) NMJ areas. Traces are on the same scale, indicated in the upper right corner. Following the end of the stimulus the fit curves for the mean $\Delta F/F$ data are also indicated for the Ib (red) and Is (green) data to show the trend in the average fluorescence during the high frequency stimulation. The bottom left movie shows all of the identified quantal event locations as they occur in the top left movie. The color of each location corresponds to the peak $\Delta F/F$ of that event. In the bottom right movie, event locations are added locally to give the local total counts. Note that the colorbar scale changes as individual sites accumulate more evoked transmission events. Spontaneous events occurring before or after the nerve stimulation are excluded from this cumulative data. Data corresponds to the example in Figures 6B, S6G-I and S6K-M.

Supplemental Movie 8. *In vivo* SynapGCaMP6f imaging at high magnification with ROI tracking and activity traces for UAS-TeTxLC, RN2-Gal4 and RN2>TeTxLC larvae (Related to Figure 7)
Multiple examples of *in vivo* NMJ activity at four dorsal muscle cells for the indicated genotypes (first UAS-TeTxLC, second RN2-Gal4 and third RN2>TeTxLC) during repeating endogenous activity bouts. Raw data on left was acquired at 260X magnification with an imaging frequency of 14 Hz and the movie playback is at 30 FPS. Scale bar is 50 μm. The ROI locations were determined by the image registration corrections and then applied to the raw data to calculate local SynapGCaMP6f activity. The corresponding $\Delta F/F$ traces are presented on the right, synchronized with the movie playback. All traces are on the same scale indicated in the upper right. Data corresponds to the example in Figures 7C-E and S7A-C.